EFFECT OF THE CAPILLARY FORCE ON THE REPOSE ANGLE OF GRANULAR MATERIALS

Z.Y. WANG[1], Y. TAN[2]

[1]Affiliation: Department of Geotechnical Engineering, College of Civil Engineering, Tongji University, Shanghai, China
E-mail address: wangziye1998@tongji.edu.cn

[2]Affiliation: Department of Geotechnical Engineering, College of Civil Engineering, Tongji University, Shanghai, China
E-mail address: tanyong21th@tongji.edu.cn

Key words: Repose Angle, Capillary Force, Liquid Bridge Model, DEM Simulation

Abstract. *The angle of repose does affect the behavior of granular materials and has a wide range of applications. The addition of a small amount of liquid can dramatically change the properties of granular media, leading to an increase in the repose angle. This change is mainly attributed to the capillary force resulting from the liquid bridge when the small amount of water was introduced. The capillary force as an attractive force increases the interaction between particles and becomes a dominant factor affecting the angle of repose because it is usually stronger than gravity. In this paper, a new discrete element method (DEM) model was developed in which the capillary force was calculated by the liquid bridge model based on toroidal approximation. The developed DEM model linked the microscopic liquid bridge volume to the macroscopic water content and it also considered the effect of liquid bridge breakage and formation on capillary force. The numerical model was first validated by comparing the experimental and numerical results. Then, the effects of surface tension, volume of the liquid bridge, and the contact angle are studied numerically. Finally, the empirical equation between water content and angle of repose is given under the present simulation conditions. This work will provide a deep understanding for the effect of capillary on the angle of repose.*

1. INTRODUCTION

The repose angle is an important parameter for understanding the micro and macro-behavior of the granular material. It is related to many applications including slope stability, avalanches, simulation model calibration and geotechnical engineering, etc[1]. For dry granular matter, a number of studies have been conducted to characterize the behavior of the repose angle. The existing research results showed that the repose angle is highly dependent on granular properties such as density, roughness, and granular characteristics such as particle size and shape, as well as the method used to measure the angle of repose[2,3,4].

However, for the repose angle of wet granular, it becomes more complicated due to the cohesive force among particles. Cohesive force, usually called the capillary force, arising from the liquid pressure and gas-liquid tension, has a significant influence on granular material behavior. For example: the sharp-featured sandcastles can be built by wet sand, while it would not be able for dry sand. Until now some studies have been performed on wet granular material. Hornbaker et al.[5] quantified the effect of adding liquid volume to a granular medium by experimental tests. They found that small quantities of liquid can dramatically change the properties of granular matter, leading to a significant increase in the repose angle. Tegzes et al.[6] investigated the effect of different liquid contents on the physical properties of granular media and observed three distinct regimes for repose angle under various liquid contents. Moreover, the relation between the repose angle and the volume of liquid was also evaluated[7]. To further investigate the mechanism of wet granular, the discrete element method (DEM) was introduced. Some DEM models incorporating the capillary force were developed to explore the character of wet granular media[8,9,10,11,12]. The shear strength, structure, and flowability of wet granular materials were also evaluated by applying these numerical models. Although previous studies have investigated the behavior of wet granular materials, limited researches were conducted on the repose angle. Furthermore, the effect of the capillary force repose angle is still obscure. However, the angle of repose of wet granular is one of the important macroscopic parameters in many fields ranging from landsides to the flowability of debris. Therefore, it is crucial to gain a fundamental understanding of the effect of capillary force on repose angle.

In this paper, both experimental tests and numerical analysis were conducted to investigate the effect of capillary force on repose angle. First, different water content tests were performed and the effects of water content on repose angle were studied. Then a DEM model incorporating the capillary force based on the "toroidal approximation" was developed. Next, a comprehensive numerical simulation was conducted. Finally an empirical equation between water content and repose angle was obtained based on the numerical results.

2. EXPERIMENTAL PROGRAM AND MATERIALS

The experiment setup aimed to investigate the repose angle of wet granular materials is shown in **Figure 1**. It consists of a 60mm diameter and 200mm height cylinder, a camera, a motor, and a 600mm×600mm horizontal wooden plane. The granular materials used in this test are glass beads (**Figure 2**) with a uniform particle size distribution ranging from 2.0mm to 2.5 mm. The density and the bulk density of the glass beads are 2500kg/m^3 and 1500kg/m^3, respectively. In this test, the hollow cylinder method was employed to determine the repose angle of wet granular materials[2]. A camera located in front of the cylinder was used to record the test process.

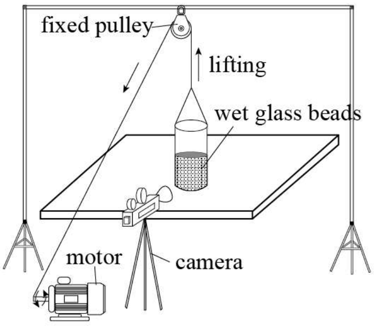

Figure 1: Schematic diagram of the experimental apparatus

Figure 2: Test materials: glass beads

The experimental procedure was as follows:

1) Weight the mass of 400g dry glass beads and pour them into a drum. Next, a certain mass of pure water was added into the drum. In this way, the various water contents ($w = m_w / m_s$) of wet granular can be obtained. It should be noted that water content of wet granular materials was limited in the range of 0 (dry) to 5%. In this range of water contents, the shape of the liquid bridge can be described by toroidal approximation[13]. The detailed experimental scheme is shown in **Table 1**. Finally, seal and start the drum to rotate for about three minutes to ensure the homogeneity of water distribution inside the glass beads.

2) The obtained wet glass beads under different water contents were filled into the cylinder and then leveled. The height of the glass beads in the cylinder was about 90mm and the aspect ratio a = 1.5 (90mm/62mm)[2]. Next, lift the cylinder slowly (the lifting velocity was 2.0cm/s) to ensure that the granular materials can form a deposit statically[14]. Then the repose angle of wet granular materials can be evaluated. To ensure the credibility of the test results, each test was repeated 4 times.

Table 1: Test conditions

Particle size (mm)	Mass of glass beads m_s (g)	Water content w (%)	Mass of water added m_w (g)
2.0 - 2.5	400	0.10; 0.25 0.50; 1.00 2.00; 3.00 4.00; 5.00	0.40; 1.00 2.00; 4.00 8.00; 12.00 16.00; 20.00

3. TEST RESULTS

3.1 The deposit morphologies

The deposit morphologies for different water content are illustrated in **Figure 3**. It can be found that there are some significant differences in the deposit morphology between the dry and wet glass beads. For wet granular materials, the final deposit looked like an "inverted bowl" whereas for dry granular materials, it looked like a "cone" (e.g. for the cases of w = 1.0% and 2.0%). Furthermore, it can also be observed that the deposit morphology transformed gradually from the "cone" to the "invert bowl" between w = 0.0% to w=1.0% (e.g. w=0.1%). Another distinctive feature is that some particles adhered to the hollow cylinder walls and remained on them for a long time. This phenomenon was also observed in similar experiments of wet particles[11,15].

3.2 Effect of water content on the repose angle

Figure 4 presents the experimental results of repose angle under different water content w. In **Figure 4**, three distinct regimes with different characteristics were observed. For the case of very low water content (w) less than 0.5% (*regime I*), the repose angle (α) is linear with w and increases sharply with w; for the case of medium w ranging from 0.5% to 3%, α is nonlinear with w and the increasing rate of α decreases gradually with w, which was defined as the *regime II*; for the case of large w (*regime III*), α remains nearly constant with w. From the experimental results, it can be concluded that the small water content would lead to a significant increase in repose angle. This is mainly due to the capillary force raised from the interstitial water among particles[9]. To further investigate the effect of capillary force on repose angle at a microscopic level and quantitatively determine the parameters affecting the repose angle, the numerical analyses were conducted later.

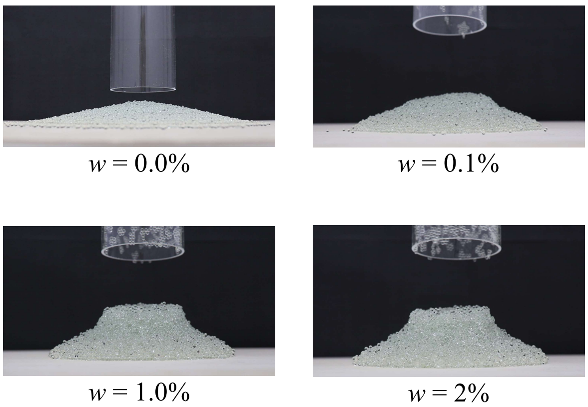

Figure 3: The deposit morphology for different water contents.

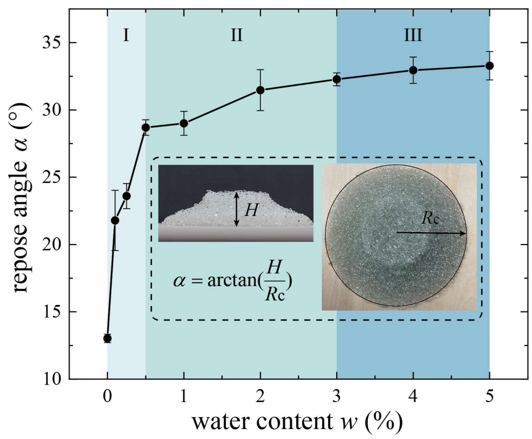

Figure 4: The experimental results of repose angle for different water content.

4. NUMERICAL ANALYSIS

In this paper, a new DEM model incorporating the capillary force was developed and the effect of capillary force on repose angle was studied. The relationship between the capillary force and repose angle was quantified based on numerical results.

4.1 Theory for modeling

The new DEM model is modified based on the rolling resistance linear contact model[16]. In the DEM model, the translational and rotation motion of the particle can be described respectively by:

$$m_i \frac{d\overrightarrow{\mathrm{v}_i}}{dt} = \sum_j (\overrightarrow{F_{ij}^{\mathrm{n}}} + \overrightarrow{F_{ij}^{\mathrm{s}}} + \overrightarrow{F_{ij}^{\mathrm{c}}}) + m_i \vec{g} \tag{1}$$

$$I_i \frac{d\overrightarrow{\omega_i}}{dt} = \sum_j (\overrightarrow{T_{ij}^{\mathrm{s}}} + \overrightarrow{T_{ij}^{\mathrm{r}}}) \tag{2}$$

where m_i, I_i, $\overrightarrow{\mathrm{v}_i}$, $\overrightarrow{\omega_i}$ are the mass, the moment of inertia, the translational and angular velocity of particle *i*, respectively; t and $\vec{g}$ represent the time and gravitational acceleration; $\overrightarrow{F_{ij}^{\mathrm{n}}}$, $\overrightarrow{F_{ij}^{\mathrm{s}}}$ and $\overrightarrow{F_{ij}^{\mathrm{c}}}$ are the normal force, shear force, and capillary force between particles *i* and *j*, respectively; $\overrightarrow{T_{ij}^{\mathrm{s}}}$ and $\overrightarrow{T_{ij}^{\mathrm{r}}}$ are the torque acting on particles, which respectively result from the shear force and rolling friction.

The modified theoretical formulas proposed by Tsunazawa et al.[16] for capillary force $\overrightarrow{F_{ij}^{\mathrm{c}}}$ based on "toroidal approximation" were adopted in this study, which were expressed as follows:

$$\overrightarrow{F_{ij}^{\mathrm{c}}} = \begin{cases} \dfrac{2\pi R\gamma\cos\theta}{1+\{[1+2V/(\pi Rh)^2]^{1/2}-1\}^{-1}} & \text{particle - particle} \\ \dfrac{4\pi R\gamma\cos\theta}{1+\{[1+2V/(\pi Rh)^2]^{1/2}-1\}^{-1}} & \text{particle - wall} \end{cases} \tag{3}$$

where γ and θ are the surface tension and the contact angle respectively; $R = 2r_i r_j/(r_i + r_j)$, r_i and r_j denote the radius of the adjacent particles *i* and *j*; *h* is the distance between particles *i* and *j*, which can be expressed by Eq. (4):

$$h = \begin{cases} h & h > \lambda R \\ \lambda R & h < \lambda R \end{cases} \tag{4}$$

where λ is the distance coefficient which can be taken as 0.1 in this paper.

V is the volume of the liquid bridge, which can be calculated by Eq. (5):

$$V = \frac{V_i}{N_i} + \frac{V_j}{N_j} \tag{5}$$

where V_i and V_j are the volume of liquid that particles *i* and *j* contain, respectively; N_i and N_j are the liquid bridge coordinate numbers of particles *i* and *j*, respectively; The relationship between V_i and water content can be considered as follows:

$$V_i = \frac{4\pi r_i^3 \rho_s w}{3N_i \rho_w} \tag{6}$$

where w is the water content; ρ_s and ρ_w are the density of particle and water ($\rho_s = 2500\mathrm{kg/m^3}$; $\rho_w = 1000\mathrm{kg/m^3}$).

The distance at which a liquid bridge breaks can be calculated using the Eq. (7) proposed by Lian[17]:

$$L_r = (1 + 0.5\theta)V^{1/3} \tag{7}$$

where L_r is the rupture distance of a liquid bridge.

4.2 Validation of the numerical model

To verify the validity of the numerical model, three-dimensional simulations consistent with the physical tests are performed. In addition, the results of numerical simulation and experiments were compared comprehensively. The parameters adopted in the DEM model are calibrated by the repose angle of dry glass beads, as shown in **Table 2**.

Table 2 Parameters used in DEM simulations

Parameters	values
Particle diameter size (mm)	2.0-2.5
Particle density (kg/m^3)	2500
Porosity (-)	0.40
Friction coefficient (-)	0.25
Rolling resistance coefficient (-)	0.24
Effective modulus (N/m^2)	1×10^6
Normal to shear stiffness ratio (-)	2.0

Figure 5 shows the results of numerical simulations under different water content. From **Figure 5**, it can be seen that the deposit morphologies of numerical simulation can match well with the experimental results. Furthermore, the comparison of the repose angle between the experimental and numerical results is shown in **Figure 6**. Combining **Figure 5** and **Figure 6**, it can be found that the numerical results based on the new DEM model were fairly well correlated with the experimental results, which proved the validity of the numerical model.

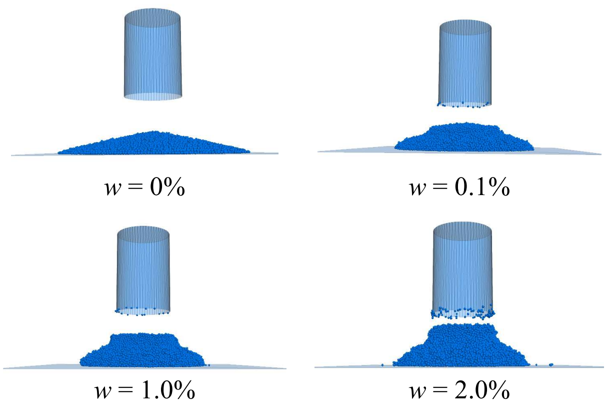

Figure 5: Numerical simulation results under different water content

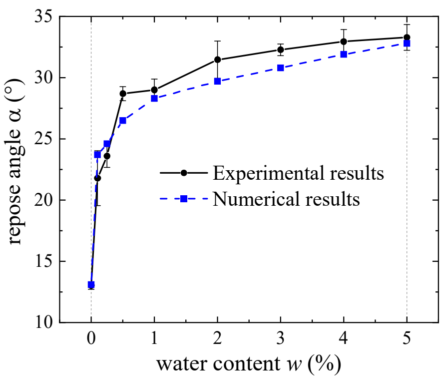

Figure 6: Comparison of experimental and numerical results

4.3 Parametric analysis

The previous researches[7,8] showed that the repose angle is related to the capillary force. The bond number Bo[18], which can be defined by Eq. (8), was used to study the relationship between the capillary force and the repose angle.

$$Bo = \frac{\overrightarrow{F_{ij}^{c}}_{\max}}{W} \tag{8}$$

Combing the Eqs. (3) and (4), the $\overrightarrow{F_{ij}^{c}}_{\max}$ in Eq. (8) can be expressed as follows:

$$\overrightarrow{F_{ij}^{c}}_{\max} = \frac{2\pi R_{\min}\gamma\cos\theta}{1+\{[1+2V/(\pi\lambda^{2}R_{\min}^{3})]^{1/2}-1\}^{-1}} \tag{9}$$

where $R_{\min}$ is the minimum particle size.

Combing Eqs. (8) and (9) leads to the equation (10):

$$Bo = \frac{\dfrac{2\pi R_{\min}\gamma\cos\theta}{1+\{[1+2V/(\pi\lambda^{2}R_{\min}^{3})]^{1/2}-1\}^{-1}}}{\dfrac{4}{3}\pi R_{\min}^{3}\rho_{s}g} = \frac{3\gamma\cos\theta}{2R_{\min}^{2}\rho_{s}g}\frac{1}{1+\{[1+2V/(\pi\lambda^{2}R_{\min}^{3})]^{1/2}-1\}^{-1}} \tag{10}$$

According to Eq. (2), the water volume in Eq. (10) can be evaluated by eq. (11)

$$V = \frac{8\pi R_{\min}^{3}\rho_{\mathrm{s}}w}{3N_{avg}\rho_{\mathrm{w}}} \tag{11}$$

where N_{avg} represents the average liquid bridge coordinate numbers, which can be taken as 6 based on the numerical results.

Substituting Eq. (11) into the Eq. (10) leads to:

$$Bo = \frac{3\gamma\cos\theta}{2R_{\min}^{2}\rho_{s}g}\frac{1}{1+\{[1+16\rho_{\mathrm{s}}w/(3\pi\lambda^{2}\rho_{\mathrm{w}}N_{avg})]^{1/2}-1\}^{-1}} \tag{12}$$

From Eq. (12), it can be found that *Bo* contains the parameters of the surface tension γ, contact angle θ, water content *w*, particle size $R_{\min}$, and the density of particle ρ_{s}. So, if we can get the relationship between the repose angle and *Bo*, the empirical equation between repose angle and these parameters mentioned above can be obtained. In light of this, we display the numerical simulation results of the repose angle under different *Bo* by changing these parameters, as shown in **Figure 7**. Furthermore, the fitting line between the repose angle and *Bo* is also given herein.

$$\alpha = 13.5 + 14.6 \times Bo^{0.32} \tag{13}$$

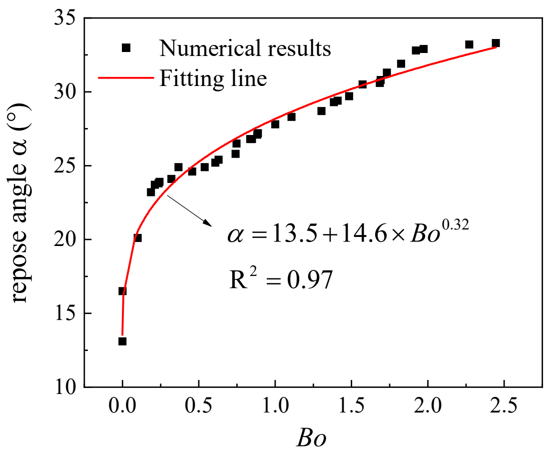

Fig 7. Numerical results of the repose angle under different *Bo*

Substituting Eq. (12) into Eq. (13), the empirical equation between the repose angle and the parameters (such as θ, γ, w, etc.) can be obtained as follows:

$$\alpha = 13.5 + 14.6 \times \left(\frac{3\gamma\cos\theta}{2R_{\min}^2\rho_s}\frac{1}{1+\{[1+16\rho_s w/(3\pi\lambda^2\rho_w N_{avg})]^{1/2}-1\}^{-1}}\right)^{0.32} \tag{14}$$

5. CONCLUSION

In this study, both the experimental tests and numerical analysis were conducted to investigate the effect of capillary force on the repose angle. Firstly, the effect of water content on the repose angle was investigated by physical experiments. Then a validated DEM model was established to study the effect of capillary force on repose angle at the microscopic level. Finally, an empirical equation used for evaluating the repose angle was proposed based on the numerical results. According to the results of experimental test, numerical simulation, and theoretical analysis, the following conclusions were drawn:

1. The experimental results show that a small water content can lead to a dramatic increase in the repose angle. The relationship between the water content (w) and the repose angle (α) can be divided into three distinct regimes. For *regime I*, α is linear with w and increases sharply with w; for *regime II*, α is nonlinear with w and the increasing rate of α decreases gradually once w reaches a certain value; for *regime III*, α increases very slowly with w and nearly keeps constant.

2. Based on the results of a validated DEM model, it is found that the repose angle is highly dependent on the *Bo*. A very low *Bo* can lead to a remarkable increase in repose angle, indicating that a small liquid can give rise to a non-negligible capillary force.

3. An empirical formula between the repose angle and water content, surface tension, contact angle, particle density, fluid density was proposed based on the numerical results.

ACKNOWLEDGEMENT

This study was supported by the National Natural Science Foundation of China (grant no. 42177179).

REFERENCES:

[1] Al-Hashemi H, Al-Amoudi O. A review on the angle of repose of granular materials. *Powder Technol*. (2018) **330**:397-417.

[2] Lajeunesse E, Mangeney-Castelnau A, Vilotte J P. Spreading of a granular mass on a horizontal plane. *Phys. Fluids*. (2004) **16**(7):2371-2381.

[3] Miura K, Maeda K, Toki S. Method of measurement for the angle of repose of sands. *Soils Found*. (1997) **37**(2):89-96.

[4] Zhou Y C, Xu B H, Yu A B, et al. An experimental and numerical study of the angle of repose of coarse spheres. *Powder Technol*. (2002) **125**(1):45-54.

[5] Hornbaker D J, Albert R, Albert I, et al. What keeps sandcastles standing? *Nature*. (1997) **387**(6635):765.

[6] Tegzes P, Albert R, Paskvan M, et al. Liquid-induced transitions in granular media. *Phys. Rev. E*. (1999) **60**(5):5823-5826.

[7] Mason T G, Levine A J, Ertas D, et al. Critical angle of wet sandpiles. *Phys. Rev. E*. (1999) **60**(5):5044-5047.

[8] Soulié F, Cherblanc F, Youssoufi M S, et al. Influence of liquid bridges on the mechanical behaviour of polydisperse granular materials. *Int. J. Numer. Anal. Methods Geomech*. (2006) **30**(3):213-228.

[9] Richefeu V, Youssoufi M S, Peyroux R, et al. A model of capillary cohesion for numerical simulations of 3D polydisperse granular media. *Int. J. Numer. Anal. Methods Geomech*. (2008) **32**(11):1365-1383.

[10] Dong K J, Zou R P, Chu K W, et al. Effect of cohesive force on the formation of a sandpile. *Powders Grains*. (2013) **1542**:646-649.

[11] Li P S, Wang D M, Wu Y S, et al. Experimental study on the collapse of wet granular column in the pendular state. *Powder Technol*. (2021) **393**:357-367.

[12] Chu X H, Zhu Z J, Wang L. Numerical investigation on the influence of water content on collapse of granular columns. *Granul. Matter*. (2023) **25**(2):37.

[13] Liu X, Zhou A N, Shen S L, et al. A micro-mechanical model for unsaturated soils based on DEM. *Comput. Meth. Appl. Mech. Eng*. (2020) **368**:113183.

[14] Liu Z. Measuring the angle of repose of granular systems using hollow cylinders. (2011) University of Pittsburgh.

[15] Gabrieli F, Artoni R, Santomaso A, et al. Discrete particle simulations and experiments on the collapse of wet granular columns. *Phys. Fluids*. (2013) **25**(10):103303.

[16] Tsunazawa Y, Fujihashi D, Fukui S, et al. Contact force model including the liquid-bridge force for wet-particle simulation using the discrete element method. *Adv. Powder Technol*. (2016) **27**(2):652-660.

[17] Lian G, Thornton C, Adams M J. A theoretical study of the liquid bridge forces between two rigid spherical bodies. *J. Colloid Interface Sci*. (1993) **161**(1):138-147.

[18] Nase S T, Vargas W L, Abatan A A, et al. Discrete characterization tools for cohesive granular material. *Powder Technol*. (2001) **116**(2-3):214-223.